Polymer Bulletin (2024) 81:1635–1649
https://doi.org/10.1007/s00289-023-04789-3

ORIGINAL PAPER

Heat diffusivity and mechanical properties of a tire bladder composite in the presence of ceramic fillers

Mehdi Shiva[1] · Mahdieh Ahmadi[2] · Elham Esmaili[3] · Morteza Zivdar[3]

Received: 5 November 2022 / Revised: 14 March 2023 / Accepted: 2 April 2023 /
Published online: 11 April 2023

Abstract

The development of a heat conductive formulation for rubber composites is essential for technical applications such as tire-curing bladders. The present study addresses the effects of three potential ceramic fillers, namely titanium carbide (TiC), silicon carbide (SiC), and alumina, on the mechanical and thermal properties of carbon black (CB)-filled butyl rubber composites. The composites were prepared using the melt compounding method. The curing, mechanical, and thermal conductivity properties of the composites were determined. The tensile strength and modulus of composites decreased slightly in the presence of ceramic fillers in lower amounts of filler loading (10 Phr). Further they reduced in a higher amount of filler loading (20 Phr). In addition, the thermal diffusivity coefficient of the composites increased in the presence of ceramic fillers with different values depending on the type and the amount of the filler with the rank of $Al_2O_3 > SiC > TiC$ at 10 Phr of filler loading and $SiC > TiC > Al_2O_3$ at 20 Phr of filler loading. These different behaviors were discussed according to the state of filler dispersion in the rubber matrix and rubber–filler interactions according to the FeSEM visualization and the mechanical properties.

Keywords Butyl rubber · Thermal diffusivity · Ceramic fillers · Phonon · Mechanical properties

✉ Mehdi Shiva
mehdishiva@birjandut.ac.ir

[1] Department of Chemical Engineering, Birjand University of Technology, P. O. Box: 97198-66981, Birjand, Iran

[2] Department of Research and Technology, Kavir Tire Co., P. O. Box 518, Birjand, Iran

[3] Department of Chemical Engineering, University of Sistan and Baluchestan, P. O. Box 98155-987, Zaheden, Iran

Introduction

Elastomers are generally low heat conductive materials due to the lack of free electrons in their structures and their strong phonon scattering characteristics. Phonons are quantized modes of vibration in a rigid crystal lattice, which are the primary thermal energy carriers in polymers, so phonon transport is considered to be the main mechanism of thermal conductivity in most polymers and rubbers [1, 2]. Amorphous rubbers are usually considered to have lots of defects in their structure that contribute to numerous phonon scatting, leading to weak thermal conductivity characteristics [3]. The incorporation of functional fillers is an effective method to improve phonon transport and thermal conductivity in amorphous rubbers [3]. According to the thermal conduction path theory as the most widely accepted thermal conduction mechanism, paths are formed by the contact of thermally conductive fillers through a polymer matrix, and the thermal energy is transmitted along thermally conductive fillers paths with lower thermal resistance [2]. Highly thermally conductive fillers such as lightweight carbon derivatives (carbon nanotubes, carbon fibers, graphite, and graphene oxide) have been investigated to upgrade the thermal conductivity of elastomers [1, 4, 5]. Ceramic fillers such as zinc oxide, boron nitride, aluminum nitride, alumina, and silicon carbide are an inorganic family of heat conductive fillers; that the opportunities and challenges for their application in rubber formulation have been recently well addressed and reviewed [1, 5].

Traditionally, tire industry curing bladders play a vital role in the vulcanization process of green tires, where the pressure and heat energy are applied to the green tire in a mold to give it its final shape and to conduct the cross-linking reaction. When the curing cycle begins bladder is inserted into the green tire from the lower mold, and heat is transferred from a recirculating heat transfer medium, such as steam, hot water, or inert gas inside the bladder [6]. Generally, bladder formulations consist of butyl rubber (and some amount of polychloroprene rubber) filled with carbon black as a reinforcing agent, castor oil as a plasticizer, and curing resins [7, 8]. Here, the thermal transport characteristics of bladder composite affect the temperature profile of different points of the tire during the curing process as well evidenced in our previous heat transfer simulation studies [9, 10]. So, a sufficient rise in bladder heat transfer coefficients can be helpful to conduct the tire-curing processes at more economical conditions. Some scientific texts have studied the increase in thermal conductivity of butyl rubber with the help of different carbon-based fillers such as carbon black, modified graphite, graphene oxide, and carbon nanotubes [11–13]. Some works of the literature also address increasing the thermal conductivity of butyl rubber with the help of ceramic fillers for non-bladder and bladder tire-curing applications [9, 10, 14, 15]. The thermal conductivity of butyl rubber has increased by using ceramic fillers such as silicon carbide [9], boehmite [10], barium titanate [14], and boron carbide [15]. In contrast to metals, in which electrons carry heat, ceramic materials transport heat mainly by phonons (the quanta of lattice waves). Hence, the thermal conductivity of ceramic fillers is primarily dependent on the mean free path

of phonons [16]. In addition to the intrinsic thermal conductivity of fillers, the filler–rubber interactions and the state of filler dispersion are significant factors that affect the phonon scattering and thermal transport properties of the rubber composites [1, 2, 4]. Filler–rubber interactions and the state of filler dispersion are also important factors that affect the mechanical properties of the composites, which are the determining factors of the service life of the bladder. TiC, SiC, and alumina are three well-known ceramic fillers with numerous industrial applications [17, 18]. Intrinsic thermal conductivity of TiC, SiC, and alumina is reported in the range of 20–25, 41–145, and 30–42 W/mK, respectively [1, 2, 5, 17]. Some publications address the application of alumina, SiC, and TiC, as potential fillers for rubber composites [19–22]. Abdel-Aziz has reported the increase in heat conductivity and thermal diffusivity of EPDM rubber in the presence of alumina microparticles [19]. Alumina fillers are attractive materials for improving the thermal conductivity properties of rubber composites and for large-scale applications, such as tire technology, as stated by Mirizzi et al. [1]. Li et al. developed thermally conductive ESBR vulcanizates with the aid of SiC fillers [23].

Thermally conductive polymer composites with different polymer matrix, various conductive fillers, and diverse fabrication methods have been well investigated and reviewed for thermal management applications [24, 25]. Polymers such as polyethylene, polypropylene, polystyrene, poly (vinyl alcohol), epoxy, nitrile–butadiene rubber, and silicon rubber have been employed as host polymers [24–27]. Conductive fillers from three different categories (metals, carbon-based, and ceramic fillers) with different particle sizes, various morphologies, diverse adapted surface characteristics, and different amounts of loading have been incorporated by different fabrication technologies to prepare heat conductive polymer composites [24–26]. The effectiveness of the filler in increasing the thermal conductivity of the polymer composite is manifested in two opposite phenomena: (1) creating an effective heat-conducting path in the polymer matrix, which favors the heat conduction of the filled composite and, (2) the thermal resistance of the filler–filler and the polymer–filler interface, which is detrimental to the thermal conductivity of the filled composite. However, the literature mainly focuses on the application of heat conductive fillers for thermal management of non-tire applications. For example, SiC and alumina have been incorporated to the epoxy and silicon rubber matrix to improve the heat conductivity of the composite for electronic packaging applications [28–31].

A review of the literature shows that no published article is available regarding the use of alumina and TiC as heat conductive fillers for large-scale applications such as tire-curing bladders. While our previous paper addresses the application of SiC in butyl rubber composite [9], it is nevertheless helpful to have a comparative study between ceramic fillers with different intrinsic thermal conductivities and dispersion states in the rubber substrate. So, here, we investigated the effects of three potential microparticle ceramic fillers, namely TiC, SiC, and alumina, on the mechanical and thermal diffusivity properties of a butyl rubber composite in the presence of carbon black. With the help of electron microscope images, it is also shown how the thermal diffusivity of butyl rubber composite is affected by the agglomeration and networking of the ceramic fillers in the rubber matrix.

Experimental

Materials

Commercial alumina powder (Al_2O_3, α-type, purity > 99%) with an average particle size of 5 µm and commercial silicon carbide powder (SiC, α-type, purity > 99%) with an average particle size of 20 µm were obtained from Tooma Co., Iran. Titanium carbide powder (TiC, purity > 99%) with the particle size of 100 µm was supplied from VEL Belgium. Butyl rubber (IIR, BK1675) was provided from Nizhnekamskneftekhim inc, Russia, and chloroprene rubber, CR(Byprene), was purchased from Arlanxeo, Germany. Carbon black (CB, N339) from Carbon Iran Co, Iran, was used as a filler. Zinc oxide and stearic acid used as activators were manufactured by Sepid Oxide Shokoohieh, Iran, and PT. Duakuda, Indonesia, respectively. Solid paraffin and castor oil used as processing aids were obtained from Kimia Zarrin, Iran, and FSG, Pacific Commodities, India, respectively. Alkyl phenol formaldehyde resin, type SP 1045 (Phenolic resin), as a curing agent, was supplied by Si Group, France.

Preparation of butyl rubber composites

Table 1 presents the bladder composite formulations used in this study. Heat conductive fillers, including TiC, SiC, and alumina microparticles, have been added to the formula in the amount of 10 and 20 Phr. The composites were prepared by using a Banbury type PL, 1.6 internal mixer (POMINI, Rubber & Plastics, Italy), and a laboratory two-roll mill type Mcc N-225X450 (Battaggion, Italy). Butyl rubber (IIR) with polychloroprene (CR) and fillers, stearic acid, solid paraffin, and castor oil were mixed in a first step in Banbury with a rotor speed of 40 rpm, for 10 min (discharge temperature of 145 to 150 °C) to produce the desired masterbatches. After mixing, the compound was taken out from the mixing chamber and sheeted out in a laboratory two-roll mixing mill with a tight nip gap and finally at a nip gap of 3 mm. In the next step of compound preparation, phenolic resin and zinc oxide were added

Table 1 Formulations of the bladder composites

Formulation (Phr)	R	TiC(10)	SiC(10)	Al2O3(10)	TiC20	SiC20	Al2O3(20)
Butyl rubber (IIR)	95	95	95	95	95	95	95
Polychloroprene (CR)	5	5	5	5	5	5	5
carbon black	60	60	60	60	60	60	60
TiC	0.0	10.0	0.0	0.0	20.0	0.0	0.0
α-SiC	0.0	0.0	10.0	0.0	0.0	20.0	0.0
α-Al_2O_3	0.0	0.0	0.0	10.0	0.0	0.0	20.0
Stearic acid	1.4	1.4	1.4	1.4	1.4	1.4	1.4
Solid paraffin	2.9	2.9	2.9	2.9	2.9	2.9	2.9
Castor oil	6.7	6.7	6.7	6.7	6.7	6.7	6.7
Phenolic resin	8	8	8	8	8	8	8
Zinc oxide	5.0	5.0	5.0	5.0	5.0	5.0	5.0

to the masterbatches on a two-roll mill, and satisfactory homogeneous stocks were obtained after 10 min of milling. All of the studied compounds were stored at room temperature for 24 h before molding. After measuring the cure properties, the butyl rubber compounds were cured at 180 °C for 50 min in a hydraulic press at a pressure of 120 kgf/cm^2 for tensile and thermal diffusivity measurements.

Material characterizations

Curing characteristics

The curing characteristics, including minimum torque (ML), maximum torque (MH), delta torque (DH), scorch time (Tc10), and curing time (Tc90) of the butyl rubber composites, were determined at 185 °C by a moving die rheometer (MDR, SMD-200B, Iran).

Tensile tests

Tensile properties of composites were monitored in terms of tensile modulus (M300) and tensile strength, according to ASTM D412, using dumbbell-shaped samples (with a thickness in the range of 1.5–2 mm and width 6.73 mm), the tests being carried out using a tensile test machine (5–10 K-S, Hounsfield, UK). The tensile test speed used was 500 mm/min. The experiment was performed with three samples, and the average results are reported.

Thermal diffusivity measurement

The details of the methodology employed for the determination of thermal diffusivity (α) of the composites are presented in the previous publications [9, 10, 32–34]. In brief, to determine α, the temperature changes were recorded at the center of a $5\times5\times2$ cm^3 cured sample (for each bladder composite) immersed in a hot viscous oil bath at temperatures of 140, 160, and 180 °C, using the temperature recorder. The temperature profile data were then used to calculate α. To do so, a combination of the heat transfer simulation using ABAQUS finite element software and a trial-and-error approach was employed. The following three-dimensional transient heat conduction was solved for a point in the center of a rectangular sample assuming constant α.

$$\frac{\partial^2 T(x,y,z,t)}{\partial x^2}+\frac{\partial^2 T(x,y,z,t)}{\partial y^2}+\frac{\partial^2 T(x,y,z,t)}{\partial z^2}=\frac{1}{\alpha}\frac{\partial T(x,y,z,t)}{\partial T} \tag{1}$$

In Eq. (1), the sample temperature (T) is based on the time variable (t), the location (x, y, z) in the Cartesian coordinates, and the thermal diffusion coefficient of the rubber composite (α).

After defining the problem in ABAQUS software, the hypothesized amount was considered for α, and the problem was solved. The simulated temperature profile in the sample center was compared with the experimental data for the thermocouple

test for the sample center. This process was repeated with different values of α so that the simulation and experimental profiles became as close as possible to each other. In this way, for each of the oil bath temperatures, a value of α was calculated, and its average was reported.

Scanning electron microscopy test

The filler morphology in rubber composite was investigated using a field emission scanning electron microscopy (FeSEM), MIRA3 FESEM/EDX (Tescan, Czech Republic). The fractured surfaces of the composite were prepared by immersion in liquid nitrogen, the test samples being surface coated with gold. The FESEM characterization and EDS mapping were employed to confirm the components and element distribution further.

Results and discussion

SEM investigations

The dispersion state of alumina, SiC, and TiC fillers is well depicted through EDS mapping of Al, Si, and Ti elements from FeSEM pictures of Fig. 1 (10 Phr loading of ceramic fillers) and Fig. 2 (20 Phr loading of ceramic fillers).

Alumina and SiC have a good state of dispersion in the rubber matrix as well depicted by element mapping of Al and Si elements, respectively. In addition, alumina particles show more compact structures compared to SiC particles at 10 Phr of loading, as shown in Fig. 1. But, SiC particles show a more compact structure in 20 Phr loading, as shown in Fig. 2. However, TiC presents with larger particles in rubber matrix, and does not form a filler network as well depicted from element mapping of Ti element.

To better investigate the distribution of alumina in the rubber matrix, Fig. 3 shows the FeSEM pictures for composites with 10 and 20 Phr of alumina in the absence of other ceramic fillers. The magnification of the image is 500x. The photographs clearly show that micron-sized agglomerates are formed in amounts of 20 Phr of alumina.

Effect of ceramic fillers on curing and tensile properties of butyl rubber composites

Table 2 presents MDR data of butyl rubber composites. Maximum torque (MH) decreases with the incorporation of ceramic fillers (TiC, SiC, and alumina), while minimum torque (ML) remains somewhat unchanged. In addition, the delta torque of the composites decreases, which implies a decrease in the cross-linking density of rubber in the presence of ceramic fillers. The curing time (Tc90) is also found to rise in the presence of ceramic fillers, while scorch time (Tc10) remains somewhat unchanged.

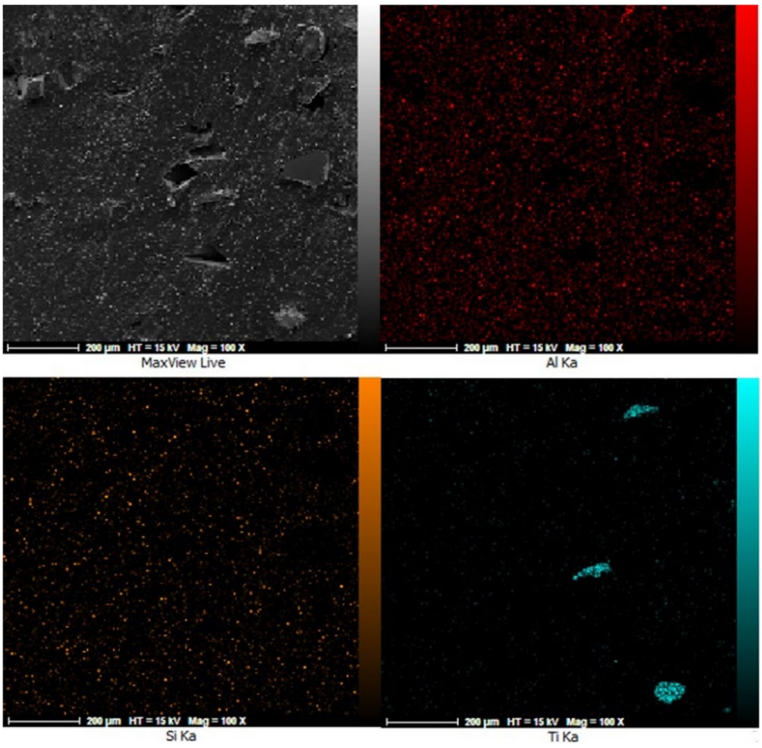

Fig. 1 FeSEM and EDS mapping of butyl rubber composites in the presence of 10 Phr of ceramic fillers. (Magnification: 100x)

Figure 4 presents the results of tensile strength and the modulus of butyl rubber composites in the presence of 10 and 20 Phr of ceramic fillers. There is a slight decrease in tensile strength in the presence of 10 Phr of ceramic fillers. Further reduction of tensile strength is observed in the amount of 20 Phr of the fillers. According to Fig. 3, the modulus values of the composites in 10 Phr of the ceramic filler do not change much, but in 20 Phr, the decrease is more noticeable. The decline in modulus can be attributed to the reduction of the cross-linking density of the butyl rubber composite in the presence of ceramic fillers. These results indicate that there is no significant interaction between ceramic fillers and rubber. So, from the mechanical viewpoint, the addition of ceramic fillers is limited to 20 Phr in the presence of carbon black at fixed values.

Effect of ceramic fillers on thermal diffusivity of carbon black-filled butyl rubber composites

Figure 5 shows that the thermal diffusivity coefficient of the composites increases in the presence of ceramic fillers, but relatively different trends are observed according to the filler type and the amount. The improvement of the thermal conductivity

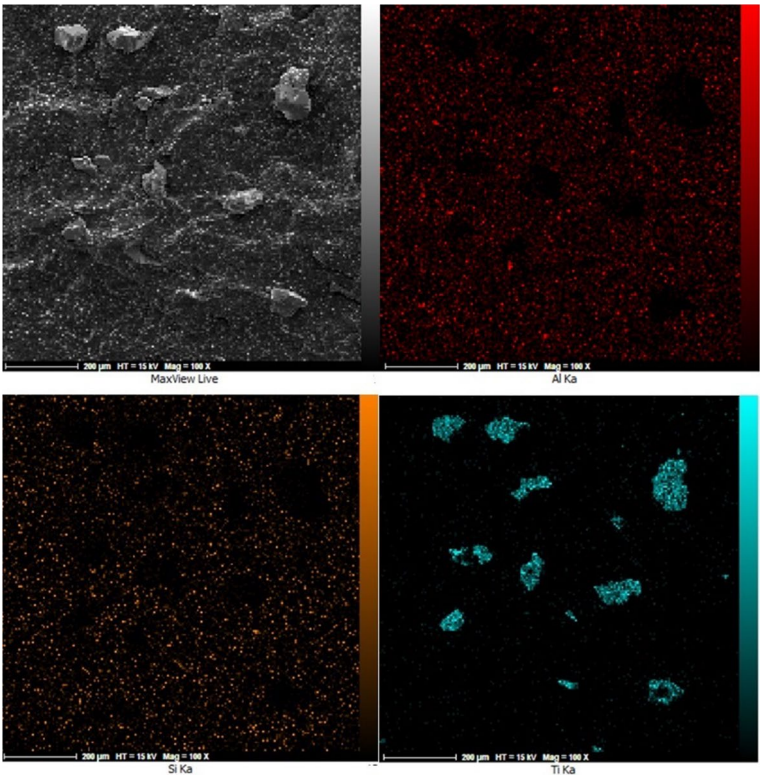

Fig. 2 FeSEM and EDS mapping of filled butyl rubber composites in the presence of 20 Phr of ceramic fillers. (Magnification: 100x)

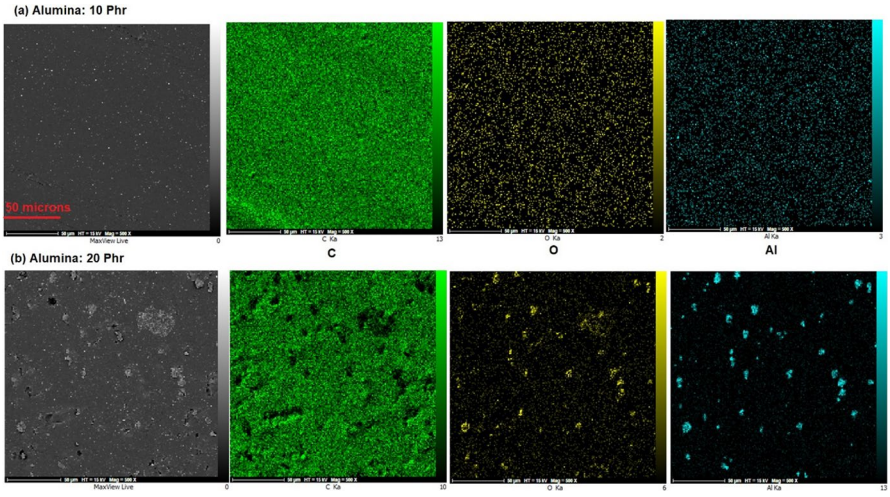

Fig. 3 FeSEM and EDS mapping of butyl rubber composites in the presence of (**a**) 10 Phr and (**b**) 20 Phr of alumina filler (Magnification: 500x)

Table 2 Curing characteristics of butyl rubber composites

Formulation	R	TiC(10)	SiC(10)	Al2O3(10)	TiC(20)	SiC(20)	Al2O3(20)
Minimum torque, ML (dN.m)	0.59 ± 0.06	0.53 ± 0.05	0.56 ± 0.02	0.56 ± 0.03	0.52 ± 0.04	0.56 ± 0.05	0.51 ± 0.05
Maximum torque, MH (dN.m)	3.06 ± 0.05	2.67 ± 0.04	2.42 ± 0.03	2.55 ± 0.04	2.31 ± 0.04	2.6 ± 0.05	2.55 ± 0.04
Delta Torque (dN.m)	2.14 ± 0.05	2.47 ± 0.04	1.86 ± 0.03	1.99 ± 0.04	1.79 ± 0.04	2.04 ± 0.05	2.04 ± 0.04
Scorch time, Tc10 (s)	89 ± 8	92 ± 7	91 ± 9	88 ± 6	97 ± 7	86 ± 7	83 ± 6
Curing time, Tc90 (s)	1560 ± 45	1680 ± 55	1573 ± 50	1657 ± 40	1606 ± 55	1573 ± 45	1642 ± 50

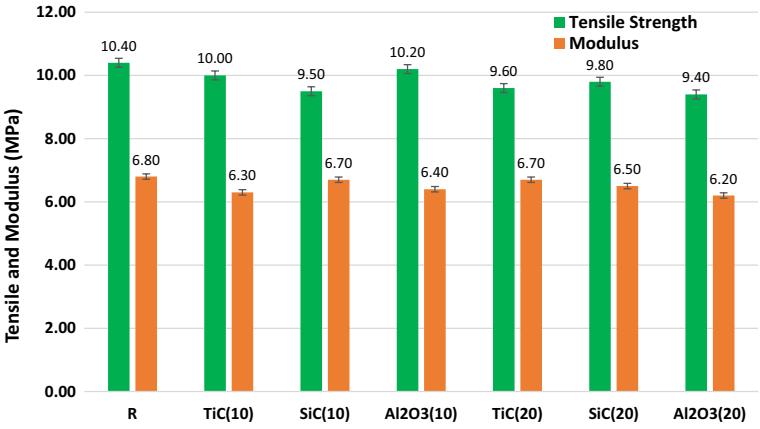

Fig. 4 The tensile strength and the modulus (300%) of butyl rubber composites in the presence of ceramic fillers

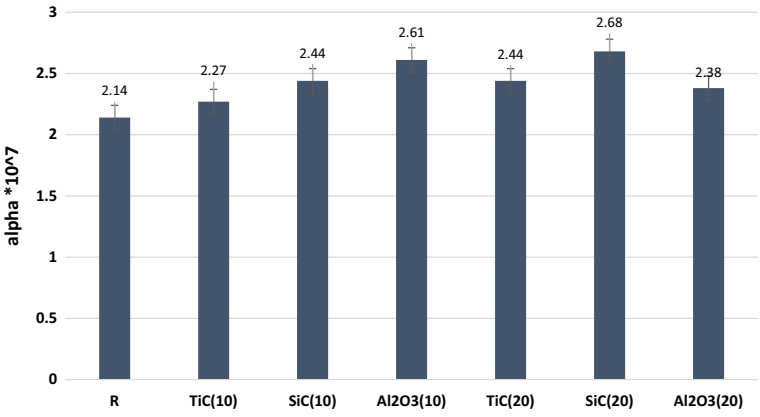

Fig. 5 Thermal diffusivities of butyl rubber composites in the presence of ceramic fillers

of butyl rubber with the help of ceramic fillers in the present study is similar to the increasing trend observed in the works of Zhou et al. [31], He et al. [35], and Cheng et al. [36], where the thermal conductivity of the rubber composite increases even with relatively small amounts of ceramic fillers. But the above studies have been done on silicone rubber matrix and in the absence of carbon black.

Titanium carbide microparticles

The thermal diffusivity coefficient of the composites increases in the presence of TiC. It has been estimated 2.27 and 2.44×10^{-7} m^2/s at 10 and 20 Phr loading of TiC, respectively. The intrinsic thermal conductivity of TiC is about 20 at room temperature, but it unusually increases with the increase in temperature and approaches

about 25 W/m.K at 200 °C [37–39]. The thermal conductivity contains both a lattice (phonon) and an electronic component in the case of TiC, and the thermal conductivity of the electronic component increases markedly with temperature [37–39]. So, an increasing trend for the thermal conductivity of TiC is observed when temperature rises. The results of Fig. 4 clearly show that the addition of 10 and 20 Phr TiC microparticles can increase the thermal diffusivity of the bladder by only about 6% and 14%, respectively. Compared to the best heat conductors such as diamond (2000 W/mK) and silver (420 W/m.K), TiC microparticles show much lower thermal conductivities due to their strong scattering of electrons and phonons by carbon vacancies of TiC in addition to the scattering of electrons by polar optical phonons and the scattering of phonons by the conduction electrons [37]. So, their incorporation in rubber shows not many effects on the thermal conductivity characteristics of the composite. In addition, the large particles of TiC that remain in the rubber substrate (Figs. 1 and 2) may play a role in intensifying the phenomenon of phonon scattering in the presence of TiC particles.

Silicon carbide microparticles

Figure 5 shows that the thermal diffusivity coefficient of the composites also increases uniformly with the increase of SiC from 2.14×10^{-7} m^2/s for 0 Phr to 2.44×10^{-7} for 10 Phr and to 2.68×10^{-7} m^2/s for 20 Phr loading of SiC. The thermal conductivity of α-SiC is about 40 W/m.K at 20 °C [37]. It decreases with the increase in temperature, and its estimated value at 200 °C is about 30 W/m.K according to the graph of thermal conductivity as a function of temperature presented in literature [40, 41]. Therefore, the thermal conductivity of SiC in the temperature range studied in this research (20–180 °C) changes only in the range of 30–40 W/m K, which is higher than the intrinsic heat conductivity of TiC (20–25 W/m.K). In addition, better filler dispersion is observed in the case of SiC rather than TiC as well shown in Figs. 1 and 2. So, SiC shows better performance rather than TiC on the thermal diffusivity of the carbon black-filled butyl rubber composite in which it is incorporated.

Alumina micro particles

While compared to the SiC, a similar range of intrinsic thermal conductivity has been reported for alumina (38–42 W/mK [1, 2]), some different trend for thermal conductivity of butyl rubber composites is observed as presented in Fig. 5. Here, the thermal diffusivity sharply increases to 2.61 in 10 Phr of alumina but it decreases to 2.38 by further increasing the amount of alumina to 20 Phr.

The FeSEM pictures may be used as a suitable tool to explain the behaviors. Alumina fillers are closer to each other in 10 Phr filler loading compared to SiC particles, according to Figs. 1 and 3a. They are well dispersed without the formation of large agglomerates, so it is expected to form better heat-conducting paths [1]. However, at 20 Phr of filler loading, some agglomerates depicted in the case of alumina fillers (Figs. 2 and 3b) can play a role in reducing the observed thermal diffusion coefficient due to the phenomenon of phonon scattering. In addition, according

to the mechanical properties of Fig. 4, the tensile and modulus of composites are more decreased in the case of 20 Phr alumina rather than SiC. So, it may be concluded that filler–rubber interaction effects and enhancement of defects in interfaces of alumina surfaces and rubber chains may play a critical role in to decrease of phonon transport and thermal conductivity ability of the filled composite at 20 Phr of alumina loading. No agglomerates are observed in 20 Phr of SiC. In this case, the particles are closer to each other and form better thermal conductive paths as well depicted in Fig. 2.

It is important to note that the mechanical properties of bladder composite do not change significantly at 10 Phr loading of alumina microparticles, so from the practical viewpoint, this composite is the best choice among the composites of the present study.

Filler morphology effects through networking and defects phenomena

A filler enters the elastomer matrix through the application of shear stresses in the melt mixing process. These stresses must be large enough to crush the coarse filler particles and distribute the fine particles well in the elastomer bed. The heat transfer through a filled elastomer composite is governed by two critical phenomena, filler networking that creates heat conductive paths and filler agglomeration and filler–rubber interface defects that dissipate heat through phonon scattering and decrease the heat conduction efficiency. Very efficient filler–rubber interaction is required to ensure a high degree of filler dispersion and networking (percolation) and the maximum reduction of the factors affecting the phonon scattering phenomenon, which includes filler agglomeration and defect areas at the filler–rubber interface [1, 2, 4]. The effect of a heat conductive filler on the heat conductivity of elastomer composites is the result of the balances of these two phenomena as well shown in the present study. In the case of TiC coarse particles, weak networking phenomena are observed at 10 and 20 Phr of loading, as evidenced through Map/EDS FeSEM images. However, more robust filler networking is observed for alumina at 10 Phr of loading and for SiC at 20 Phr of loading, as a result of good breakdown and distribution/dispersion of these fillers. Finally, filler defects through weak filler–rubber interaction (interface defects) and agglomeration are an undesirable phenomenon that harms the heat conduction behavior of the rubber composite. These effects are well demonstrated in the present study at 20 Phr of alumina loading as well as our previous study at 28 Phr of SiC loading [9].

It should be noted that the thermal diffusion coefficient of the carbon black-filled butyl rubber of present study has improved by only 5–25% in the presence of ceramic fillers. For practical purposes, larger amounts of improvement are probably needed. Using ceramic fillers with different particle sizes and morphologies along with improving the interfacial adhesion between filler and matrix by modifying the particle surface, hybridizing with other types of conductive fillers to create more efficient heat conductive networks in rubber matrix can be considered for future studies [1, 42, 43]. The synergistic effects in increasing the thermal conductivity of polymer composites by using ceramic fillers with different particle sizes (micron and sub-micron) in combination with each other have been reported for both alumina

[29] and SiC [44]. These studies can also be done for butyl rubber composite. Better improving in the thermal conductivity of silicone rubber have been reported using spherical and branched alumina particles [36, 42] as well as SiC whiskers [31]. The use of such fillers with more effective morphologies can be beneficial for butyl rubber-based tire-curing bladder applications.

Conclusions

The results of the present study revealed that the thermal diffusivity coefficient of carbon black-filled butyl rubber composite increases using heat conductive fillers such as TiC, SiC, and alumina microparticles. However, the filler dispersion, the filler network formation (percolation), the filler agglomeration, and filler interface defects are essential aspects that determine the efficiency of the filler on heat transport properties of elastomer composite. SiC and alumina show better dispersion state and networking effects, hence better efficiency rather than TiC on thermal diffusivity coefficients. As an adverse phenomenon on the heat transfer properties of the elastomeric composite, agglomeration and the weak filler–rubber interaction of alumina particles in 20 Phr of use is well addressed in this article. Therefore, by using the ceramic fillers of this study, it is possible to increase the thermal diffusion coefficient of bladder composite only to a limited amount.

Acknowledgements The authors greatly appreciate the support of Kavir Tire Company.

Declarations

Conflict of interest The authors declare that they have no known competing financial interests or personal relationships that could have appeared to influence the work reported in this paper.

References

1. Mirizzi L, Carnevale M, D'Arienzo M, Milanese C, Di Credico B, Mostoni S, Scotti R (2021) Tailoring the thermal conductivity of rubber nanocomposites by inorganic systems: opportunities and challenges for their application in tires formulation. Molecules 26:3555
2. Guo Y, Ruan K, Shi X, Yang X, Gu J (2020) Factors affecting thermal conductivities of the polymers and polymer composites: a review. Compos Sci Technol 193:108134
3. Li A, Zhang C, Zhang Y (2017) Thermal conductivity of graphene-polymer composites: mechanisms, properties and applications. Polymers 9:437
4. Guo B, Tang Z, Zhang L (2016) Transport performance in novel elastomer nanocomposites: mechanism, design and control. Prog Polym Sci 61:29–66
5. Niu H, Ren Y, Guo H, Małycha K, Orzechowski K, Bai S (2020) Recent progress on thermally conductive and electrical insulating rubber composites: design, processing and applications. Compos Commun 22:100430
6. Deniz V, Karaagac B, Ceyhan N (2007) Thermal stability of Butyl/EPDM/Neoprene based rubber compounds. J Appl Polym Sci 103:557–563
7. Ivan G, Buqaru E, Volintiru T (1988) A new activation system for resin curing of butyl rubber. Acta Polym 39:647–651
8. Samadi A, Razzaghi Kashani M (2010) Effects of organo-clay modifier on physical–mechanical properties of butyl-based rubber nano-composites. J Appl Polym Sci 116:2101–2109

9. Shiva M, Kamkar Dallakeh M, Ahmadi M, Lakhi M (2021) Effects of silicon carbide as a heat conductive filler in butyl rubber for bladder tire curing applications. Mater Today Commun 29:102773
10. Shiva M, Lakhi M, Robat AS (2019) Increase heat conductivity of bladder and calculate its effect on temperature profile of the tire in the curing process. Appl Res Chem—Polym Eng 3:93–105
11. Nasr GM, Badawy MM, Gwaily SE, Shash NM, Hassan HH (1995) Thermophysical properties of butyl rubber loaded with different types of carbon black. Polym Degrad Stab 48:237–241
12. Bian H, Xue J, Hao G, Hao Y, Xie M, Wang C, Wang Z, Zhu L, Xiao Y (2021) High thermal conductivity graphene oxide/carbon nanotubes/butyl rubber composites prepared by a dry ice expansion pre-dispersion flocculation method. J Appl Polym 139:e51897
13. Malas A, Das CK (2017) Influence of modified graphite flakes on the physical, thermo-mechanical and barrier properties of butyl rubber. J Alloy Compd 699:38–46
14. Gwaily SE, Nasr GM, Badawy MM, Hassan HH (1995) Thermal properties of ceramic-loaded conductive butyl rubber composites. Polym Degrad Stab 47:391–395
15. Meng D, Wang N, Li G (2014) Electric heating property from butyl rubber loaded boron carbide composites. J Wuhan Univ Technol-Mater Sci Ed 29:492–497
16. Babapoor A, Shahedi Asl M, Ahmadi Z, Sabahi Namini A (2018) Effects of spark plasma sintering temperature on densification, hardness and thermal conductivity of titanium carbide. Ceram Int 44:14541–14546
17. Pierson HO (1996) Handbook of refractory carbides and nitrides, Properties, Characteristics, In: Processing and Applications, NOYES Publications, USA
18. Hart L, Lense E (1990) Alumina chemicals: science and technology handbook. Wiley-American Ceramic Society, USA
19. Abdel-Aziz MM, Gwaily SE, Madani M (1998) Thermal and electrical behavior of radiation vulcanized EPDM/Al_2O_3 composites. Polym Degrad Stab 62:587–597
20. Chameswary J, Namitha LK, Brahmakumar M, Sebastian MT (2014) Material characterization and microwave substrate applications of alumina-filled butyl rubber composites. Int J Appl Ceram Technol 11:919–926
21. Guntur NPR, Yadav SG, Gopalan S (2020) Effect of titanium carbide as a filler on the mechanical properties of styrene butadiene rubber. Mater Today: Proc 24:1552–1560
22. Yadav SG, Guntur NPR, Rahulan N, Gopalan S (2021) Effect of titanium carbide powder as a filler on the mechanical properties of silicon rubber. Mater Today: Proc 46:665–671
23. Li Z, Chen H, Zhu Z, Zhang Y (2011) Study on thermally conductive ESBR vulcanizates. Polym Bull 67:1091–1104
24. Zhang F, Feng Y, Feng W (2020) Three-dimensional interconnected networks for thermally conductive polymer composites: design, preparation, properties, and mechanisms. Mater Sci Eng R 142:100580
25. Xu Y, Wang X, Hao Q (2021) A mini review on thermally conductive polymers and polymer-based composites. Compos Commun 24:100617
26. Leung SN (2018) Thermally conductive polymer composites and nanocomposites: processing-structure-property relationships. Compos B Eng 150:78–92
27. Yang D, Kong X, Ni Y, Gao D, Yang B, Zhu Y, Zhang L (2019) Novel nitrile-butadiene rubber composites with enhanced thermal conductivity and high dielectric constant. Compos A 124:105447
28. Song J, Wu L, Zhang Y (2020) Thermal conductivity enhancement of alumina/silicone rubber composites through constructing a thermally conductive 3D framework. Polym Bull 77:2139–2153
29. Wang ZY, Zhou XN, Li ZX, Xu SS, Hao LC, Zhao JP, Wang B, Yang JF, Ishizaki K (2021) Enhanced thermal conductivity of epoxy composites by constructing thermal conduction networks via adding hybrid alumina filler. Polym Compos 43:483–492
30. Yang K, Gu M (2010) Enhanced thermal conductivity of epoxy nanocomposites filled with hybrid filler system of triethylenetetramine-functionalized multi-walled carbon nanotube/silane-modified nano-sized silicon carbide. Compos A 41:215–221
31. Zhou W, Wang C, An Q, Ou H (2008) Thermal properties of heat conductive silicone rubber filled with hybrid fillers. J Compos Mater 42:173–187
32. Shiva M, Akhtari SS, Shayesteh M (2020) Effect of mineral fillers on physico-mechanical properties and heat conductivity of carbon black-filled SBR/butadiene rubber composite. Iran Polym J 29:957–974
33. Shiva M, Lakhi M (2019) Studying the effects of silica/alumina and silica/boehmite binary filler on the mechanical properties and the non-isothermal curing time of carbon black filled tyre tread composite. Compos Part B 175:107124

34. Ghoreishy M, Naderi G, Pahlavan M (2016) An investigation into the thermal transport properties of PP/EPDM/clay nanocomposites using a new combined experimental/numerical method. Plast, Rubber Compos 45:229–237
35. He Y, Chen ZC, Ma LX (2010) Thermal conductivity and mechanical properties of silicone rubber filled with different particle sized SiC. Adv Mater Res 87–88:137–142
36. Cheng JP, Liu T, Zhang J, Wang BB, Ying J, Liu F, Zhang XB (2014) Influence of phase and morphology on thermal conductivity of alumina particle/silicone rubber composites. Appl Phys A 117:1985–1992
37. Pierson H O (1996) Carbides of group IV: titanium, zirconium, and hafnium carbides. Handbook of refractory carbides and nitrides. Chapter 4:55-80
38. Williams Wendell S (1998) The thermal conductivity of metallic ceramics. Therm Manag, Overv 50:62–66
39. Morelli DT (1991) Thermal conductivity and thermoelectric power of titanium carbide single crystals. Phys Rev B 44:5453–5458
40. Vasilos T, Kingery WD (1954) Thermal conductivity: XI, conductivity of some refractory carbides and nitrides. J Am Ceram Soc-Vasilos Kingery 37:409–414
41. Pierson HO (1996) Carbides of group IV: titanium, characteristics and properties of silicon carbide and boron carbide. Handbook of refractory carbides and nitrides. Chapter 8: pp 137-154
42. Ouyang Y, Li X, Tian H, Bai L, Yuan F (2021) A novel branched Al_2O_3/Silicon rubber composite with improved thermal conductivity and excellent electrical insulation performance. Nanomaterials 11:2654
43. Zhuang C, Tao R, Liu X, Zhang L, Cui Y, Liu Y, Zhang Z (2021) Enhanced thermal conductivity and mechanical properties of natural rubber-based composites co-incorporated with surface treated alumina and reduced graphene oxide. Diam Relat Mater 116:108438
44. Wang Q, Gao W, Xie Z (2003) Highly thermally conductive room-temperature vulcanized silicone rubber and silicone Grease. J Appl Polym Sci 89:2397–2399